Dyes and Pigments 185 (2021) 108896

Contents lists available at ScienceDirect

Dyes and Pigments

journal homepage: http://www.elsevier.com/locate/dyepig

A quinoline-based chromogenic and ratiometric fluorescent probe for selective detection of Mg^{2+} ion: Design, synthesis and its application in salt lake brines and bioimaging

Zhen-Hai Fu [a,b,d,*], Jing-Can Qin [a,b], Ya-Wen Wang [c,**], Yu Peng [c], Yong-Ming Zhang [a,b,d], Dong-Mei Zhao [a,b,d], Zhi-Hong Zhang [a,b,d]

[a] Key Laboratory of Comprehensive and Highly Efficient Utilization of Salt Lake Resources, Qinghai Institute of Salt Lakes, Chinese Academy of Sciences, Xining, 810008, People's Republic of China
[b] Key Laboratory of Salt Lake Resources Chemistry of Qinghai Province, Xining, 810008, People's Republic of China
[c] School of Life Science and Engineering, Southwest Jiaotong University, Chengdu, 610031, People's Republic of China
[d] Innovation Academy for Green Manufacture, Chinese Academy of Sciences, Beijing, 100049, People's Republic of China

ARTICLE INFO

Keywords:
Ratiometric fluorescence
Fluorescent probe
Quinoline
Mg^{2+}ion
Salt lake brines

ABSTRACT

A fluorescent probe was rational designed and prepared to distinguish Mg^{2+} ion from Ca^{2+} ion, in which 8-hydroxyquinoline acted as not only a fluorophore but also a recognition group. Notably, this probe **QB** (8-hydroxyquinoline-5-benzothiazole) shows two fluorescence response modes for highly selective detection of Mg^{2+} ion, namely fluorescence ratiometric mode and turn-on mode, which can be realized by controlling the excitation wavelength at 356 nm or 425 nm. After the addition of Mg^{2+} ion, the color of the **QB** solution changed from colorless to yellow, which can be easily found by naked eye. All experimental results suggested that probe **QB** has a high selectivity toward Mg^{2+} ion in the presence of other cations. Its detection limit for Mg^{2+} ion was estimated as low as 0.142 μM, and this value was far lower than the intracellular concentration (0.5–1.2 mM). The detection mechanism was proposed further by the experiment of ^{1}H NMR titration and theoretical calculation. More significantly, this probe was successfully used to detect Mg^{2+} ion in brine samples as a quantitative method, and was also applied to detecting and imaging Mg^{2+} ion in living cells, indicating its great application value in practical use for the detection of Mg^{2+} ion.

1. Introduction

As one of the most important divalent cations in living beings and environments, Mg^{2+} ion is not only involved in numerous physiological activities such as cell membrane stabilization, adenosine triphosphate (ATP) utilization, stabilization of nucleotides, and cell proliferation, but also contributes to the productivity and quality of agriculture as a nutrient element [1–5]. Abnormal levels of Mg^{2+} ion can lead to various diseases, such as hypocalcaemia, hypermagnesemia, metabolic syndrome, hypertension, nausea, diarrhea, Alzheimer's disease and so on [6–11]. Significantly, Mg^{2+} ion is widely distributed in seawater, rivers and salt lakes, causing it to naturally spread throughout the environment. Specially in salt chemical industry, evaporative crystallization is currently the most effective way to utilize salt lake resources, and the evaporation rate is mainly associated with the concentration of Mg^{2+} ion [12]. In addition, the presence of Mg^{2+} ion also will increase the difficulty to extract lithium from the salt lake brines due to their similar ionic radii and chemical properties [13,14]. Therefore, it is highly desirable to detect the presence of Mg^{2+} ion in aqueous solution with reliable and efficient way.

In view of its importance, the detection of Mg^{2+} ion has attracted increasing attention in the past few years. A series of analytical techniques for detecting it have appeared, including atomic absorption spectrometry with flame (FAAS), inductively coupled plasma optical emission spectroscopy (ICP-OES), titration techniques, optical techniques and so on [15–17]. Among them, the method using a fluorescent

* Corresponding author. Key Laboratory of Comprehensive and Highly Efficient Utilization of Salt Lake Resources, Qinghai Institute of Salt Lakes, Chinese Academy of Sciences, Xining, 810008, People's Republic of China.
** Corresponding author.
E-mail addresses: fzh@isl.ac.cn (Z.-H. Fu), ywwang@swjtu.edu.cn (Y.-W. Wang).

https://doi.org/10.1016/j.dyepig.2020.108896
Received 30 August 2020; Received in revised form 25 September 2020; Accepted 27 September 2020
Available online 1 October 2020

probe became popular because of the advantages such as high reliability, real-time application, simplicity, low detection limits, low cost and the ability to be applied in real samples [18].

So far, there were limited reports about the fluorescent probe for the detection of Mg^{2+} ion compared to other cations. Even though some fluorescent probes have been developed for detecting Mg^{2+} ion by using compounds such as the derivatives of β-diketone [19–21], carboxylic acid [22,23], schiff base [24–33], crown ether [34,35], salicylalde-hyde [36,37], 8-hydroxyquinoline [38], porphyrin [39] and calix[4]arene [40]. As summarized in Table S1, compounds based on schiff base or crown ether can selectively detect Mg^{2+} ion in organic solvents such as ethanol, acetonitrile, isopropyl alcohol, THF and DMSO [24–32,34,35]. And the selectivity toward Mg^{2+} ion is easily interfered by Ca^{2+} ion [29–31,34,35]. In contrast, other derivatives of salicylaldehyde, 8-hydroxyquinoline, β-diketone or carboxylic acid can exhibit higher selectivity toward Mg^{2+} ion than Ca^{2+} ion in aqueous solution, but their detection limits for Mg^{2+} are not presented or not low enough [19–23, 37]. Moreover, it should be noted that these probes are all based on chelation-enhanced fluorescence (CHEF) and show fluorescence turn-on response to Mg^{2+} ion by using fluorescence changes at only one wavelength, which is usually problematic for practical use. To the best of our knowledge, there were several ratiometric fluorescent probes for Mg^{2+} ion [24,39,40], but they have also some disadvantages, such as the lack of detailed information for sensing Mg^{2+} ion, complicated structure, no comparison with Ca^{2+} ion or high detection limit. Consequently, the development of probes with multi-output fluorescence signals special for Mg^{2+} ion remains a challenge.

In connection with our continuing research of chromogenic and ratiometric fluorescent probe for the detection of different analytes [41], herein, we report a new quinoline-based fluorescent probe **QB** (Fig. 1), in which 8-hydroxyquinoline served as not only a fluorophore but also a recognition group. By modification with a benzothiazole group, the weak luminescence properties of 8-hydroxyquinoline caused by the PPT (Intermolecular Photoinduced Proton Transfer) process can be effectively improved. After the formation of complex between **QB** and Mg^{2+} ion, the PPT process was inhibited and the detection of Mg^{2+} ion with fluorescence ratiometric changes can be realized. Finally, the rapid, high selective, chromogenic and ratiometric detection of Mg^{2+} ion over Ca^{2+} ion was successfully achieved in an aqueous solution.

2. Experimental

Detailed information of chemicals and materials, spectra measurement could be found in the Supplementary data.

2.1. Synthesis of 8-hydroxyquinoline-5-carbaldehyde (Q-5-CHO)

This procedure was adapted from a known literature with minor changes [42]. 8-hydroxyquinoline (14.5 g, 0.1 mol) and EtOH (70 mL) were added to a 500 mL three-neck round-bottom flask at room temperature. The resulting mixture was stirred for 10 min after the addition of a mixture of NaOH aqueous solution (100 g, 37%). The color changed to yellow along with the formation of some solid products, then dissolved the solid by heating to 110 °C in an oil bath. $CHCl_3$ (20 mL) was added dropwise while the reaction temperature was maintained at 75 °C. The reaction mixture was further stirred for 10 h at 70 °C, and then cooled to room temperature. The pH value was adjusted to about 7.0 with HCl (1 M), and the khaki precipitate appeared. This solid was filtered and purified by flash column chromatography (PET/EtOAc = 5:1) on silica gel to afford the crude 8-hydroxyquinoline-5-carbalde-hyde, which could be recrystallized in acetone to give pure sample (3.57 g, 20%) as a pink crystal solid. m.p.: 174.7–175.9 °C. ^{1}H NMR (DMSO-d_6, 400 MHz) δ = 11.17 (s, 1H), 10.13 (s, 1H), 9.55 (dd, J = 8.4, 1.6 Hz, 1H), 8.97 (dd, J = 4.0,1.6 Hz, 1H), 8.16 (d, J = 8.4 Hz, 1H), 7.78 (dd, J = 8.8, 4.4 Hz, 1H), 7.25 (d, J = 8.0 Hz, 1H) ppm. ^{13}C NMR (DMSO-d_6, 100 MHz) δ = 192.2, 159.6, 148.9, 140.3, 138.0, 133.1, 126.8, 124.6, 122.4, 110.9 ppm. ESI−MS: m/z 174.1 $[M + H]^+$.

2.2. Synthesis of probe *QB* (8-hydroxyquinoline-5-benzothiazole)

QB was synthesized according to a previous reported method with minor modifications [43]. HCl (37%, 1.0 mL, 12.0 mmol) and H_2O_2 (30%, 2.4 mL, 24.0 mmol) were added to a solution of 2-aminothiophe-nol (0.64 mL, 6.0 mmol) and 8-hydroxyquinoline-5-carbaldehyde (693 mg, 4.0 mmol) in EtOH (30 mL). The resulting mixture was stirred at r.t. for 90 min, and then quenched by 300 mL H_2O. The precipitate was filtered, dried under vacuum and recrystallized from CH_2Cl_2-EtOH to afford the desired product (620 mg, 56% yield). m.p.: 180.9–182.0 °C. ^{1}H NMR (DMSO-d_6, 400 MHz) δ = 10.68 (s, 1H), 9.72 (d, J = 8.8 Hz, 1H), 8.98 (d, J = 4.0 Hz, 1H), 8.08–8.17 (m, 3H), 7.77 (dd, J = 8.8, 4.4 Hz, 1H), 7.57 (t, J = 8.0 Hz, 1H), 7.48 (t, J = 8.0 Hz, 1H), 7.24 (d, J = 8.0 Hz, 1H) ppm. ^{13}C NMR (DMSO-d_6, 100 MHz) δ = 166.9, 156.3, 153.8, 148.7, 138.5, 134.6, 133.9, 132.0, 126.5, 126.2, 125.4, 123.4, 122.8, 121.9, 119.8, 111.2 ppm. ESI−MS: m/z 279.1 $[M + H]^+$.

2.3. Synthesis of compound *NB* (*4*-benzothiazole-1-naphthol)

HCl (37%, 0.25 mL, 3.0 mmol) and H_2O_2 (30%, 0.6 mL, 6.0 mmol) were added to a solution of 2-aminothiophenol (0.32 mL, 3.0 mmol) and 4-hydroxy-1-naphthaldehyde (344 mg, 2.0 mmol) in EtOH (15 mL), The resulting mixture was stirred at r.t. for 90 min, then the solution was added to 100 mL H_2O, and followed by extraction with EtOAc (40 mL × 3). The combined organic phase was dried by anhydrous Na_2SO_4. The solvent was removed by evaporation, and the residue was purified by flash column chromatography (petroleum ether/EtOAc = 10:0.5–10:1) on silica gel to afford **NB** as the desired solid (391.6 mg, 70.6% yield). m. p.: 210.3–211.8 °C. ^{1}H NMR (DMSO-d_6, 400 MHz) δ = 11.04 (s, 1H), 9.20 (d, J = 8.4 Hz, 1H), 8.29 (d, J = 8.0 Hz, 1H), 8.12 (t, J = 8.0 Hz, 2H), 7.95 (d, J = 8.4 Hz, 1H), 7.66–7.70 (m, 1H), 7.53–7.60 (m, 2H), 7.44–7.48 (m, 1H), 7.04 (d, J = 8.0 Hz, 1H) ppm. ^{13}C NMR (DMSO-d_6, 100 MHz) δ = 167.9, 156.4, 153.9, 134.2, 131.6, 131.3, 128.1, 126.4, 125.6, 125.5, 125.2, 124.7, 122.7, 122.6, 121.8, 120.5, 107.9 ppm. ESI−MS: m/z 278.1 $[M + H]^+$.

2.4. Cell cytotoxicity assay

The toxicity of probe **QB** in Hela cells was evaluated by a traditional CCK-8 assay. HeLa cells (5×10^3) were first seeded into a 96-well plate,

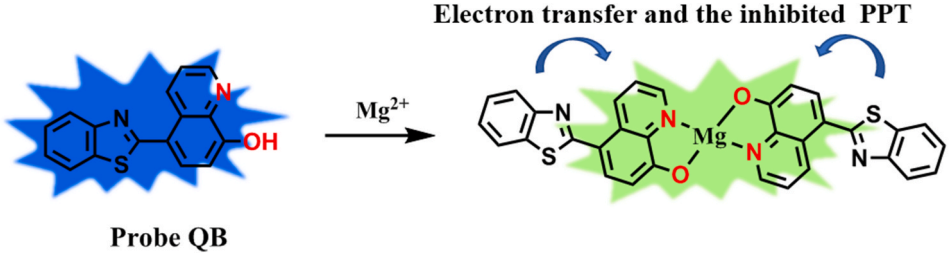

Fig. 1. Our fluorescent probe for Mg^{2+} ion.

then various of probe **QB** (0, 2.0, 5.0, 10.0, 15.0, 20.0 μM) was added and incubated at 37 °C in a final volume of 100 μL. Kept this condition for 24 h, CKK-8 (10 μL) was added to every well and continue to be incubated for another 3 h at 37 °C. The absorbance at 450 nm was performed on a Bio-Tek Synergy HT Multi-Mode Microplate Reader.

2.5. Cell culture and imaging

HeLa cells in the experiment were cultured in DMEM (10% FBS, 100 units/mL penicillin and 100 units/mL streptomycin) under an atmosphere of 5% CO_2 and 95% air at 37 °C. The cells were seeded at a density of 3×10^5 and incubated at 37 °C for 24 h. Before the experiment, the culture medium was replaced with new DMEM. First, the cells were incubated with 0.4 mM, 4.0 mM, and 8.0 mM Mg^{2+} for 1h, respectively. Then the cells were washed three times by using PBS buffer solution to remove excess Mg^{2+} present in the extracellular medium, and the culture medium was subsequently replaced with new DMEM. Finally, these cells were cultured in the presence of probe **QB** (10.0 μM) for further 1 h, then the cells were washed three times using PBS buffer solution. The bright filed and fluorescence images were obtained using a Leica-SP5 confocal microscope (λ_{ex} = 405 nm, λ_{em} = 500–580 nm), the temperature of cells was kept at 37 °C with a Tokai Hit-GSI controller.

3. Results and discussion

3.1. Design and syntheses of probes

As mentioned in our previous work [41], one characteristic of a visual and ratiometric fluorescent probe should be able to emit fluorescence at a different wavelength after the addition of analyte. It is well known that 8-hydroxyquinoline are usually poor luminescent due to its PPT (Intermolecular Photoinduced Proton Transfer) process between the hydroxyl group and the nitrogen group [44]. To solve this problem, aldehyde group was introduced to 8-hydroxyquinoline by using a Reimer-Tiemann reaction, which can be further used to prepare probe bearing benzothiazole group.

Scheme 1 shows the route for the synthesis of probe **QB**. 8-hydroxyquinoline-5-carbaldehyde was first prepared, and then the reaction of 8-hydroxyquinoline-5-carbaldehyde with 2-aminothiophenol resulted in the formation of probe **QB**. For a control experiment, we also prepared a compound **NB** by the similar way, in which 4-hydroxy-1-naphthaldehyde was used instead of 8-hydroxyquinoline-5-carbaldehyde. The single crystal structure of probe **QB** was obtained from DMSO solution (Scheme 1). All compounds were characterized by ^1H, ^{13}C NMR, melting point, IR and mass spectra (Figs. S1–S11, see the supporting information).

3.2. UV–vis and fluorescence response of probe *QB* toward Mg^{2+} ion

As a ratiometric fluorescence probe, the fluorescence characteristic of **QB** was initially investigated in different solvents and the results were shown in Fig. S12. After excited at 356 nm, **QB** showed a strong fluorescence peak at 450 nm in dimethyl sulfoxide (DMSO), isopropanol, ethanol, N, *N*-dimethylformamide and methanol. The intensity of the emission peak was different in different solvent, which should be attributed to the disruption of intramolecular hydrogen bond in these solvents [45]. Notably, a fluorescence peak at 534 nm was also observed in N, *N*-dimethylformamide, acetonitrile and acetone, which happened presumably due to its dimer form linked by the intramolecular hydrogen bond N … •H–O [46], which inhabited the PPT process, resulting in a longer maximal emission wavelength. This result was also can be supported by the control substrate **NB**, which showed only one emission peak at about 450 nm in all above solvents (Fig. S13). Considering the practical application, the effect of water content on the fluorescence intensity of **QB** at 450 nm was further investigated. As shown in Fig. S14, with the increase of water, the fluorescence intensity decreased gradually. To make sure that **QB** can show a good ratiometric fluorescence change for the detection of analyte, a mixture of DMSO and HEPES (4-(2-hydroxyethyl)-1-piperazinethanesulfonic acid) buffer (9:1 (v/v)) was selected. Meanwhile, **QB** showed good fluorescence response to Mg^{2+} ion in the pH range from 6.0 to 9.0 (Fig. S15). Therefore, the subsequent experiments were carried out in DMSO-HEPES buffer (pH = 7.0, 9:1 (v/v)).

Consequently, the absorption spectra of probe **QB** were carried out in DMSO-HEPES buffer (pH = 7.0, 9:1 (v/v)). As demonstrated in Fig. 2, **QB** showed two absorption peaks at about 290 nm and 356 nm, respectively. With the increase in amount of Mg^{2+} ion, the intensity of absorption peak at 290 nm decreased gradually, whereas two new absorption peaks appeared and increased simultaneously at 245 nm and 425 nm, along with the changes in appearance color from colorless to yellow, which can be observed by naked eye (Fig. S16). These results indicated that a new complex was formed between probe **QB** and Mg^{2+} ion.

To further investigate the interrelation between probe **QB** and Mg^{2+} ion, the fluorescence spectra response of probe **QB** to Mg^{2+} ion was performed by using two excitation wavelengths at 356 nm and 425 nm, respectively. As illustrated in Fig. 3a and Fig. S17, under the excitation at 356 nm, the solution of **QB** exhibited blue fluorescence, and a relatively stable fluorescence emission peak was observed at 450 nm, which can be attributed to the enol form of **QB**. Notably, with the treatment of Mg^{2+} ion, the fluorescence intensity at 450 nm disappeared, and a new fluorescence peak was observed at 534 nm accompanied by an appearance of yellow-green fluorescence, which ascribed to the fluorescence emission of complex between probe **QB** and Mg^{2+} ion. In

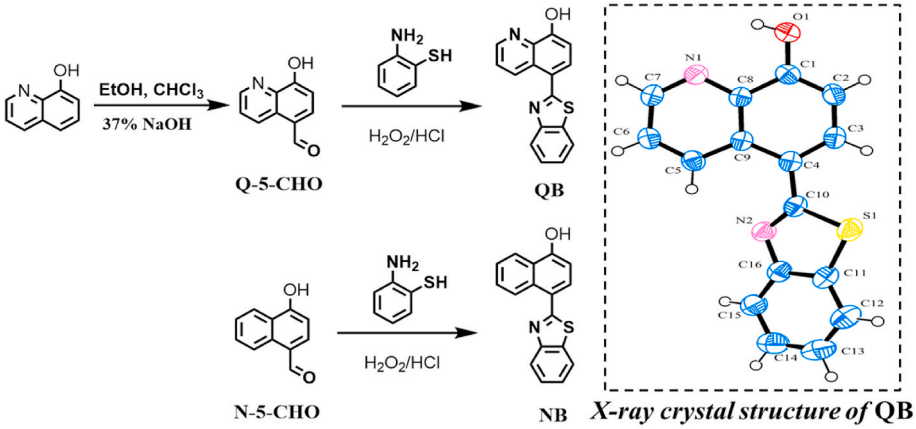

Scheme 1. Syntheses of probes.

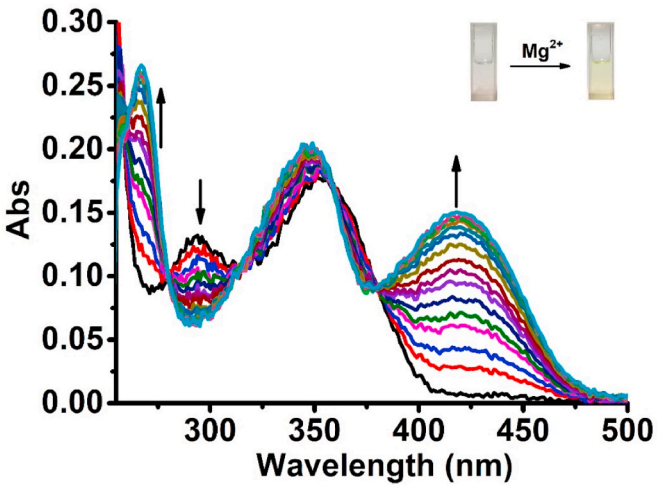

Fig. 2. UV–vis spectra of probe **QB** (10.0 μM) with Mg^{2+} ion (0–4.0 mM) in DMSO-HEPES buffer (pH = 7.0, 9:1 (v/v)).

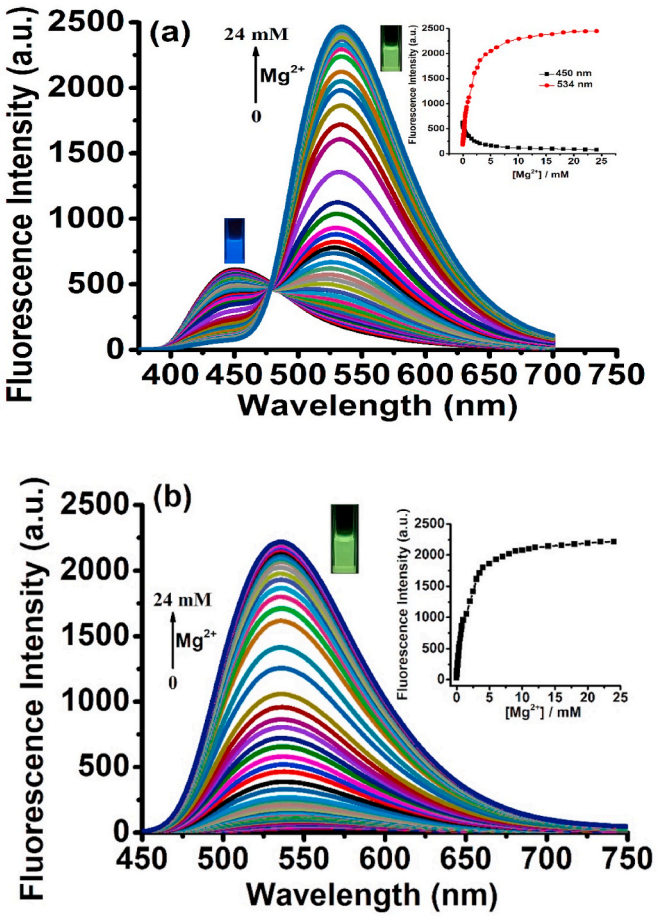

Fig. 3. Fluorescence spectral changes of probe **QB** (10.0 μM) with the addition of Mg^{2+} ion (0–24.0 mM) in DMSO-HEPES buffer (pH = 7.0, 9:1 (v/v)). (a) Inset: Fluorescence intensity of I_{534} and I_{450} changes upon the addition of Mg^{2+} ion (λ_{ex} = 356 nm). (b) Inset: Fluorescence intensity changes at 534 nm upon the addition of Mg^{2+} ion (λ_{ex} = 425 nm).

addition, there was a good linear relationship between the ratio of fluorescence intensity at 534 nm/450 nm and Mg^{2+} concentration (0–100.0 μM), the detection limit was calculated to be 0.439 μM based on the equation DL = 3σ/k (S/N = 3) (Fig. S18) [47]. Therefore, probe **QB** successfully served as a ratiometric fluorescent probe toward Mg^{2+} ion, which is superior to the reported probes with only one fluorescence emission peak (Table S1).

Separately, probe **QB** was no fluorescent when excited at a long wavelength of 425 nm, and an obvious fluorescence enhancement appeared at about 534 nm upon the addition of Mg^{2+} ion. As depicted in Fig. 3b, with the addition of Mg^{2+} ion to the solution of **QB**, the fluorescence intensity at 534 nm increased gradually and reached to the maximum value when 4.0 mM of Mg^{2+} ion was added. There was a good linear relationship between the fluorescence intensity of 534 nm and the amount of Mg^{2+} ion in the range from 0 to 25.0 μM. And the corresponding detection limit was estimated as low as 0.142 μM based on the equation DL = 3σ/k (S/N = 3) (Fig. S19) [47], which is superior to some reported results (Table S1). The rapid response time also demonstrated that probe **QB** is highly sensitive to Mg^{2+} ion (Fig. S20). The Job's plot revealed the formation of a 2:1 stoichiometric complex between **QB** and Mg^{2+} ion (Fig. S21) [48]. Apparently, these changes in the fluorescence spectra showed that probe **QB** can be used to detect Mg^{2+} ion in aqueous solution through not only a ratiometric mode but also a fluorescence "off-on" mode.

3.3. Fluorescence selectivity of probe *QB*

To further understand the selectivity of probe **QB** toward Mg^{2+} ion, the fluorescence responses of **QB** (10.0 μM) toward different metal ions were performed accordingly. As illustrated in Fig. 4, with the addition of metal cations such as Li^+, Na^+, K^+, Rb^+, Cs^+, Mg^{2+}, Ca^{2+}, Ba^{2+}, Sr^{2+}, Ni^{2+} and Mn^{2+}, the fluorescence intensity at 450 nm decreased and a new emission peak appeared at 534 nm only upon the addition of Mg^{2+} ion when excited at 356 nm. While the excitation wavelength was changed to 425 nm, the significant fluorescence enhancement was observed only in the presence of Mg^{2+} ion. However, the fluorescence change was also observed in the presence of some ions such as Al^{3+}, $Zn^{2+}$and Cd^{2+}, which indicated that the detection of Mg^{2+} by probe **QB** should be performed in the absence of these ions (Fig. S22). Specifically, probe **QB** almost showed no response toward Ca^{2+} ion.

Next, the competitive experiments in the presence of other tested metal ions were carried out to reveal the influence of other metal ions on the interaction between probe **QB** and Mg^{2+} ion. As shown in Fig. 4c and d, upon the addition of Mg^{2+} ion into the solution of **QB** and other interfering metal ions such as Li^+, Na^+, K^+, Rb^+, Cs^{2+}, Ca^{2+}, Ba^{2+}, Sr^{2+}, Ni^{2+} and Mn^{2+}, negligible disturbance was observed when excited by 356 nm or 425 nm, which indicated that these coexistent metal ions had no remarkable influence in the detection of Mg^{2+} ion. And **QB** could act as a good ratiometric and turn on fluorescent probe for the detection of Mg^{2+} ion in aqueous solution. Meanwhile, probe **QB** is highly selective toward Mg^{2+} ion over the above metal ions, especially Ca^{2+} ion.

3.4. Proposed sensing mechanism

In order to confirm the binding modes between **QB** and Mg^{2+}, ^1H NMR spectra were employed to explain the behavior of **QB** in the presence of Mg^{2+} ion. As shown in Fig. 5, H_a and H_1 are the proton signals of moiety in **QB**. With the addition of Mg^{2+} ion to the system, their signals shifted downfield clearly. And H_a disappeared in the presence of adequate Mg^{2+} ion, which indicated that the hydroxyl group is probably involved in the formation of complex between **QB** and Mg^{2+} ion. Moreover, the control substrate **NB** is insensitive to Mg^{2+} ion in fluorescence spectra (Fig. S23). By comparing their molecular structures, Mg^{2+} ion should coordinate with –OH and –N groups in **QB**.

3.5. Theoretical calculations

For a better understanding of the behavior of **QB** toward Mg^{2+} ion, DFT (density functional theory) studies were performed for optimizing the structures by using the Gaussian 09 program with B3LYP/6-311G(d)

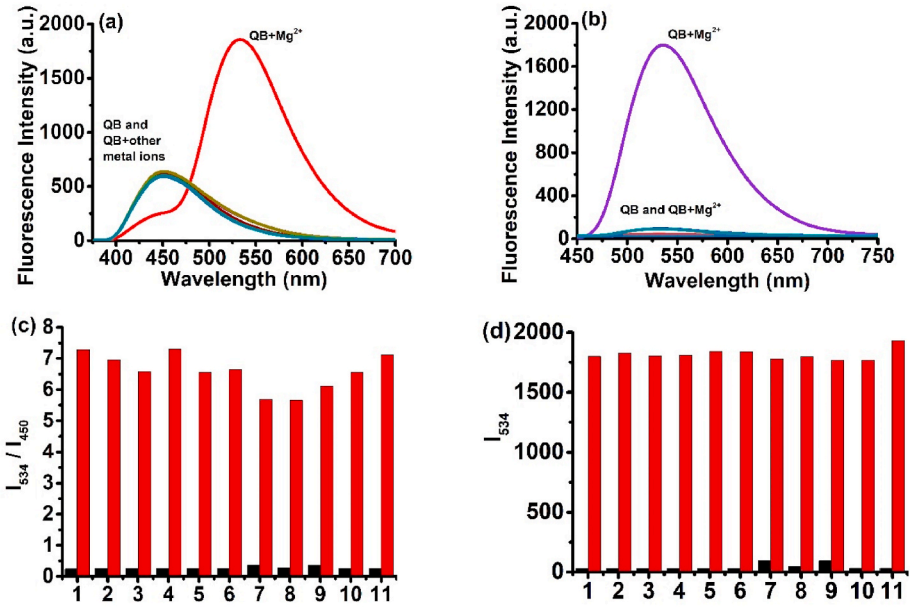

Fig. 4. Fluorescence responses of probe **QB** (10.0 μM) toward various metal ions: (a) λ_{ex} = 356 nm; (b) λ_{ex} = 425 nm. Selectivity of probe **QB** (10.0 μM): (c) λ_{ex} = 356 nm; (d) λ_{ex} = 425 nm. The black bars represent the emission intensity of probe **QB** in the presence of other ions; the red bars represent the emission intensity that occurs upon the subsequent addition of 4.0 mM Mg^{2+} ion to the above solution. From 1 to 11: only **QB**, 4.0 mM for Li^{+}, Na^{+}, K^{+}, Rb^{+}, Cs^{+}, Ca^{2+}, Ba^{2+}, Sr^{2+}, 10.0 μM for Ni^{2+} and Mn^{2+}. (For interpretation of the references to color in this figure legend, the reader is referred to the Web version of this article.)

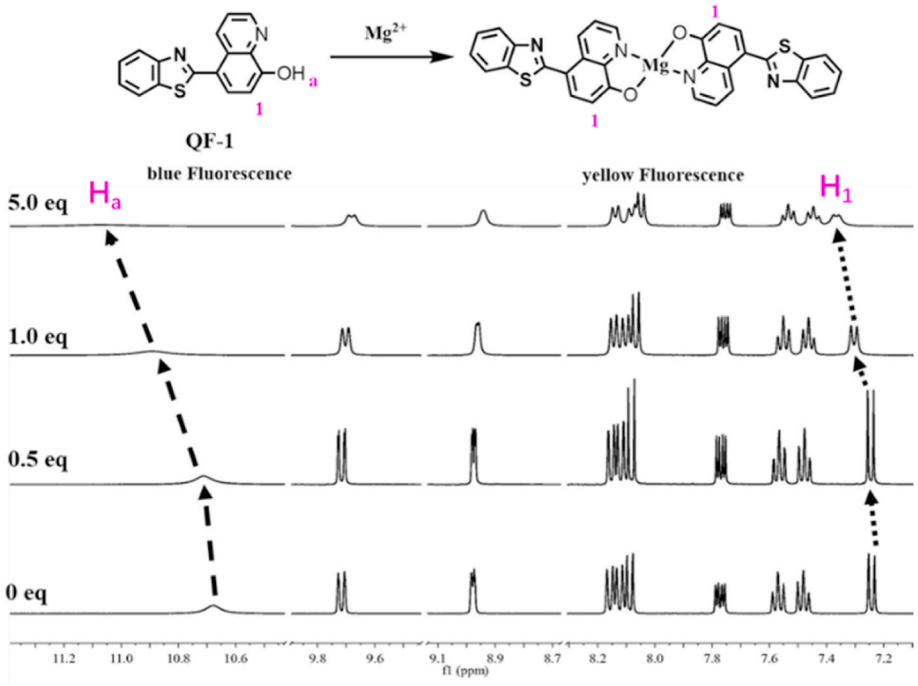

Fig. 5. Partial ^{1}H NMR spectra (400 MHz) of **QB** with Mg^{2+} ion in DMSO-d_6.

basis set [49]. As demonstrated in Fig. 6, for free **QB**, it is electron rich and the electron densities of both HOMOs and LUMOs are mainly distributed at the whole skeleton, which indicated that probe itself can exhibit fluorescence. However, after the formation of a 2:1 stoichiometric complex between **QB** and Mg^{2+} ion, the electron density on the LUMO transferred from the benzothiazole moiety to quinoline of the complex, and mainly concentrated on around Mg^{2+} ion, which was attributed to a LMCT process. Consequently, the complex showed a strong fluorescence at a longer excited wavelength due to the smaller energy gap of 2**QB** + Mg^{2+} system.

3.6. Analysis of Mg^{2+} ion in brine samples

Since **QB** exhibited good sensibility and selectivity toward Mg^{2+} ion in aqueous solution, it was used as probe to evaluate Mg^{2+} ion in real samples. It is well known that the salt lake brine is mainly composed of alkali metal and alkaline earth metal ions. Consequently, the determination of Mg^{2+} ion by using **QB** was carried out in different source of brines, such as laguocuo salt lake, da chaidam salt lake and west taijinar salt lake. As shown in Table 1, there were three methods for detecting Mg^{2+} ion, namely titration with EDTA, ICP-OES and our method, respectively. Method 1 and 2 are currently mainly used in practical application [50]. By comparing the measured concentration of Mg^{2+} ion, our method is in good agreement with that of other two methods.

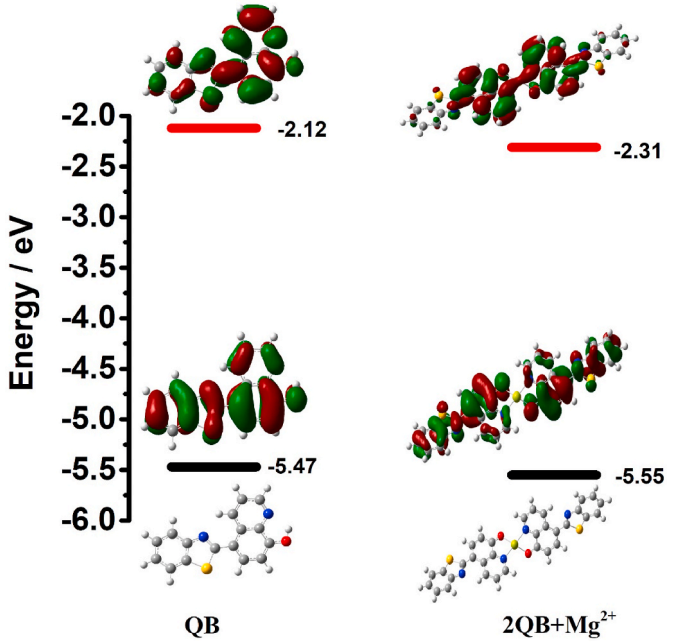

Fig. 6. Optimized structures, HOMO−LUMO energy levels, and the molecular orbital plots of **QB** and 2**QB** + Mg^{2+}.

Table 1
Comparison of different methods for Mg^{2+} ion detection in brine samples (g/L).

Sample	Method 1	Method 2	Method 3
Sample 1	0.70	0.67	0.71
Sample 2	10.81	10.07	10.49
Sample 3	23.30	23.11	23.28

Samples: 1. Laguocuo salt lake brine; 2. Da chaidam salt lake brine; 3. West taijinar salt lake brine.
Methods: 1. The concentration of Mg^{2+} ion was determined with a precision of within ±0.3% in mass fraction by titration with an EDTA standard solution in the presence of the indicator Eriochrome Black-T; 2. ICP-OES; 3. Our method.

Therefore, the analysis results suggested that **QB** can be an excellent tool to quantitatively detect Mg^{2+} ion content and have a good potential application in practice.

3.7. Fluorescence imaging of Mg^{2+} in HeLa cells

To further show its ability to be applied in biology, the detection of Mg^{2+} using probe **QB** was carried out in HeLa cells. Initially, a CKK-8 assay was employed to evaluate the cytotoxicity of probe **QB** in HeLa cells, the cells was cultured in the presence of 0, 2.0, 5.0, 10.0, 15.0, 20.0 μM probe **QB** for 24 h. As demonstrated in Fig. S24, **QB** showed low cytotoxicity to these cells and it could be used in biological fluorescent imaging. First, HeLa cells was incubated with only **QB** for 1 h, and no obvious fluorescence was observed due to the lack of DMSO in cell culture medium, which also indicated that the effect of small amount of Mg^{2+} ion in culture medium was negligible (Fig. S25). Next, HeLa cells was incubated with 0.4 mM, 4.0 mM, and 8.0 mM of Mg^{2+} ion for 1 h, respectively. As shown in Fig. 7, these cells almost showed no fluorescence, then probe **QB** (10.0 μM) was added and incubated for another 1 h, the yellow fluorescence was observed compared to the cells without **QB**, and the fluorescence intensity increased with increasing concentration of Mg^{2+} ion. Therefore, these results further suggested that probe **QB** is permeable and can be applied in bioimaging for Mg^{2+} ion in living cells.

4. Conclusions

In summary, a quinoline-based chromogenic and ratiometric probe **QB** was rationally designed for the detection of Mg^{2+} ion. In the presence of tested metal ions, it exhibited high selectivity toward Mg^{2+} ion over other tested cations. With the treatment of Mg^{2+} ion, fluorescence ratiometric and turn-on responses were observed by using two different excited wavelengths. And the detection limit was estimated as low as 0.142 μM. The color of **QB** solution changed from colorless to yellow, which can be easily observed by naked eye. ^{1}H NMR spectra and computational studies further explained the origin of the fluorescence changes. Finally, probe **QB** was successfully applied to detect Mg^{2+} ion in brine samples as a quantitative method, and was also successfully applied to detect and image Mg^{2+} ion in HeLa cells. We think this strategy would be favorable for developing fluorescence probes for other analytes.

CRediT authorship contribution statement

Zhen-Hai Fu: Investigation, Methodology, Data curation, Writing - original draft. **Jing-Can Qin:** Investigation, Software, Writing - review & editing. **Ya-Wen Wang:** Supervision, Writing - review & editing. **Yu Peng:** Supervision, Writing - review & editing. **Yong-Ming Zhang:** Supervision, Project administration. **Dong-Mei Zhao:** Supervision, Project administration. **Zhi-Hong Zhang:** Project administration.

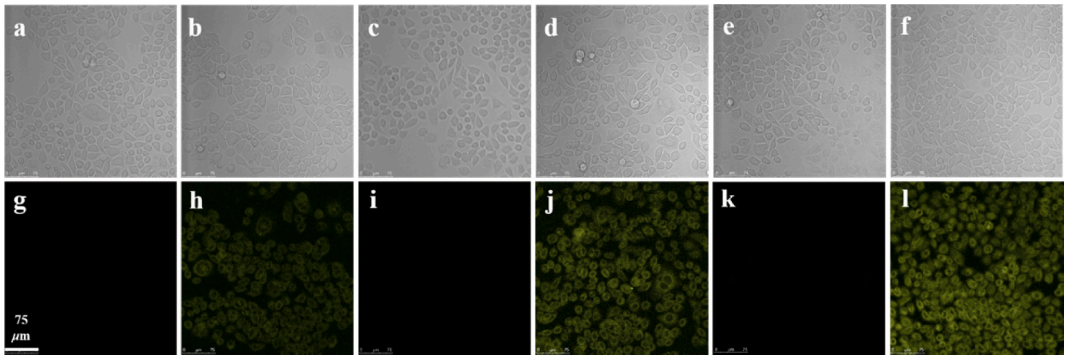

Fig. 7. HeLa cell images: (a) bright field and (g) fluorescence images of HeLa cells with Mg^{2+} (0.4 mM) for 1h; (b) bright field and (h) fluorescence images of HeLa cells incubated with Mg^{2+} (0.4 mM) for 1 h, and then incubated with probe **QB** (10.0 μM) for 1 h; (c) bright field and (i) fluorescence images of HeLa cells with Mg^{2+} (4.0 mM) for 1h; (d) bright field and (j) fluorescence images of HeLa cells incubated with Mg^{2+} (4.0 mM) for 1h, and then incubated with probe **QB** (10.0 μM) for 1 h; (e) bright field and (k) fluorescence images of HeLa cells with Mg^{2+} (8.0 mM) for 1h; (f) bright field and (l) fluorescence images of HeLa cells incubated with Mg^{2+} (8.0 mM) for 1 h, and then incubated with probe **QB** (10.0 μM) for 1 h. Scale bar = 75 μm.

Declaration of competing interest

The authors declare that they have no known competing financial interests or personal relationships that could have appeared to influence the work reported in this paper.

Acknowledgment

We thank the Natural Science Foundation of Qinghai Province (Grant Nos. 2019-ZJ-954Q), the Youth Innovation Promotion Association CAS (2018466, Y810081023) and the CAS "Light of West China" Program (Y810041019).

Appendix A. Supplementary data

Supplementary data to this article can be found online at https://doi.org/10.1016/j.dyepig.2020.108896.

References

[1] Tomita A, Zhang M, Jin F, Zhuang W, Takeda H, Maruyama T, Osawa M, Hashimoto K, Kawasaki H, Ito K, Dohmae N, Ishitani R, Shimada I, Yan Z, Hattori M, Nureki O. ATP-dependent modulation of MgtE in Mg^{2+} homeostasis. Nat Commun 2017;148.
[2] Yin J, Hu Y, Yoon J. Fluorescent probes and bioimaging: alkali metals, alkaline earth metals and pH. Chem Soc Rev 2015;44:4619–44.
[3] Fujii T, Shindo Y, Hotta K, Citterio D, Nishiyama S, Suzuki K, Oka K. Design and synthesis of a FlAsH-type Mg^{2+} fluorescent probe for specific protein labeling. J Am Chem Soc 2014;136:2374–81.
[4] Liu M, Yu X, Li M, Liao N, Bi A, Jiang Y, Liu S, Gong Z, Zeng W. Fluorescent probes for the detection of magnesium ions (Mg^{2+}): from design to application. RSC Adv 2018;8:12573–87.
[5] Peng H-Y, Qi Y-P, Lee J, Yang L-T, Guo P, Jiang H-X, Chen L-S. Proteomic analysis of Citrus sinensis roots and leaves in response to long-term magnesium-deficiency. BMC Genom 2015;16:253.
[6] Treadwell R, Moliner FD, Subiros-Funosas R, Hurd T, Knox K, Vendrell M. A fluorescent activatable probe for imaging intracellular Mg^{2+}. Org Biomol Chem 2018;16:239–44.
[7] Matsui Y, Sadhu KK, Mizukami S, Kikuchi K. Highly selective tridentate fluorescent probes for visualizing intracellular Mg^{2+} dynamics without interference from Ca^{2+} fluctuation. Chem Commun 2017;53:10644–7.
[8] Gupta VK, Mergu N, Kumawat LK, Singh AK. Selective naked-eye detection of Magnesium (II) ions using a coumarin-derived fluorescent probe. Sens Actuators, B 2015;207:216–23.
[9] Zhao L, Liu Y, He C, Wang J, Duan C. Coordination-driven nanosized lanthanide 'Molecular Lanterns' as luminescent chemosensors for the selective sensing of magnesium ions. Dalton Trans 2014;43:335–43.
[10] Hariharan PS, Anthony SP. Selective fluorescence sensing of Mg^{2+} ions by Schiff base chemosensor: effect of diamine structural rigidity and solvent. RSC Adv 2014;4:41565–71.
[11] Sargenti A, Farruggia G, Malucelli E, Cappadone C, Merolle L, Marraccini C, Andreani G, Prodi L, Zaccheroni N, Sgarzi M, Trombini C, Lombardo M, Lotti S. A novel fluorescent chemosensor allows the assessment of intracellular total magnesium in small samples. Analyst 2014;139:1201–7.
[12] Zhang J. Theoretical model and dynamics study of highly concentrated brine evaporation in solar pond. J Salt Lake Res 2000;8:22–31.
[13] Díaz Nieto CH, Palacios NA, Verbeeck K, Prévoteau A, Rabaey K, Flexer V. Membrane electrolysis for the removal of Mg^{2+} and Ca^{2+} from lithium rich brines. Water Res 2019;154:117–24.
[14] Zhang Y, Hu Y, Wang L, Sun W. Systematic review of lithium extraction from salt-lake brines via precipitation approaches. Miner Eng 2019;139:105868.
[15] Friese K-C, Krican V. Analysis of silicon nitride powders for Al, Cr, Cu, Fe, K, Mg, Mn, Na, and Zn by slurry-sampling electrothermal atomic absorption spectrometry. Anal Chem 1995;67:354–9.
[16] Trapani V, Farruggia G, Marraccini C, Iotti S, Cittadini A, Wolf FI. Intracellular magnesium detection: imaging a brighter future. Analyst 2010;135:1855–66.
[17] Lvova L, Goncalves CG, Natale CD, Legin A, Kirsanov D, Paolesse R. Recent advances in magnesium assessment: from single selective sensors to multisensory approach. Talanta 2018;179:430–41.
[18] Hamilton GRC, Sahoo SK, Kamila S, Singh N, Kaur N, Hyland BW, Callan JF. Optical probes for the detection of protons, and alkali and alkaline earth metal cations. Chem Soc Rev 2015;44:4415–32.
[19] Yin H, Zhang B, Yu H, Zhu L, Fang Y, Zhu M, Guo Q, Meng X. Two-photon fluorescent probes for biological Mg^{2+} detection based on 7-substituted coumarin. J Org Chem 2015;80:4306–12.
[20] Murata O, Shindo Y, Ikeda Y, Iwasawa N, Citterio D, Oka K, Hiruta Y. Near-infrared fluorescent probes for imaging of intracellular Mg^{2+} and application to multi-color imaging of Mg^{2+}, ATP, and mitochondrial membrane potential. Anal Chem 2020;92:966–74.
[21] Komatsu H, Iwasawa N, Citterio D, Suzuki Y, Kubota T, Tokuno K, Kitamura Y, Oka K, Suzuki K. Design and synthesis of highly sensitive and selective fluorescein-derived magnesium fluorescent probes and application to intracellular 3D Mg^{2+} imaging. J Am Chem Soc 2004;126:16353–60.
[22] Matsui Y, Funato Y, Imamura H, Miki H, Mizukami S, Kikuchi K. Visualization of long-term Mg^{2+} dynamics in apoptotic cells using a novel targetable fluorescent probe. Chem Sci 2017;8:8255–64.
[23] Komatsu H, Miki T, Citterio D, Kubota T, Shindo Y, Kitamura Y, Oka K, Suzuki K. Single molecular multianalyte (Ca^{2+}, Mg^{2+}) fluorescent probe and applications to bioimaging. J Am Chem Soc 2005;127:10798–9.
[24] Marimuthu P, Ramu A. A ratiometric fluorescence chemosensor for Mg^{2+} ion and its live cell imaging. Sens Actuators, B 2018;266:384–91.
[25] Xu J, Zheng W, Huang X, Cheng Y, Shen P. Selective fluorescent probe based on Schiff base derived from hydroxymethyl coumarin and aminated Sudan I dye for Mg^{2+} detection. Arabian J. Chem. 2017;10:S2729–35.
[26] Zhang H, Yin C, Liu T, Chao J, Zhang Y, Huo F. Selective "off-on" detection of magnesium (II) ions using a naphthalimide-derived fluorescent probe. Dyes Pigments 2017;146:344–51.
[27] Wang G-Q, Qin J-C, Fan L, Li C-R, Yang Z-Y. A turn-on fluorescent sensor for highly selective recognition of Mg^{2+} based on new Schiff's base derivative. J Photochem Photobiol A 2016;314:29–34.
[28] Liu Z, Xu H, Chen S, Sheng L, Zhang H, Hao F, Su P, Wang W. Solvent-dependent "turn-on'' fluorescence chemosensor for Mg^{2+} based on combination of C=N isomerization and inhibition of ESIPT mechanisms. Spectrochim Acta, Part A 2015;149:83–9.
[29] Yu T, Sun P, Hu Y, Ji Y, Zhou H, Zhang B, Tian Y, Wu J. A novel and simple fluorescence probe for detecting main group magnesium ion in HeLa cells and Arabidopsis. Biosens Bioelectron 2016;86:677–82.
[30] Pandey A, Kumar A, Vishwakarma S, Upadhyay KK. A highly specific 'turn-on' fluorescent detection of Mg^{2+} through a xanthene based fluorescent molecular probe. RSC Adv 2016;6:6724–9.
[31] Kao M-H, Chen T-Y, Cai Y-R, Hu C-H, Liu Y-W, Jhong Y, Wu A-T. A turn-on Schiff-base fluorescence sensor for Mg^{2+} ion and its practical application. J Lumin 2016;169:156–60.
[32] Liu Z, Xu H, Song C, Huang D, Sheng L, Shi R. A simple fluorescent chemosensor for Mg^{2+} based on C=N isomerization with highly selectivity and sensitivity. Chem Lett 2011;40:75–7.
[33] Alam R, Mistri T, Katarkar A, Chaudhuri K, Mandal SK, Khuda-Bukhsh AR, Das KK, Ali M. A novel chromo-and fluorogenic dual sensor for Mg^{2+} and Zn^{2+} with cell imaging possibilities and DFT studies. Analyst 2014;139:4022–30.
[34] Tian M, Ihmels H, Ye S. Fluorimetric detection of Mg^{2+} and DNA with 9-(alkoxyphenyl)benzo[b]quinolizinium derivatives. Org Biomol Chem 2012;10:3010–8.
[35] Hama H, Morozumi T, Nakamura H. Novel Mg^{2+}-responsive fluorescent chemosensor based on benzo-15-crown-5 possessing 1-naphthaleneacetamide moiety. Tetrahedron Lett 2007;48:1859–61.
[36] Adhikari S, Ghosh A, Guria S, Sarkar S, Sahana A. Naturally occurring thymol based fluorescent probes for detection of intracellular free Mg^{2+} ion. Sens Actuators, B 2016;236:512–9.
[37] Men G, Chen C, Zhang S, Liang C, Wang Y, Deng M, Shang H, Yang B, Jiang S. A real-time fluorescent sensor specific to Mg^{2+}: crystallographic evidence, DFT calculation and its use for quantitative determination of magnesium in drinking water. Dalton Trans 2015;44:2755–62.
[38] Marraccini C, Farruggia G, Lombardo M, Prodi L, Sgarzi M, Trapani V, Trombini C, Wolf FI, Zaccheroni N, Iotti S. Diaza-18-crown-6 hydroxyquinoline derivatives as flexible tools for the assessment and imaging of total intracellular magnesium. Chem Sci 2012;3:727–34.
[39] Ishida M, Naruta Y, Tani F. A porphyrin-related macrocycle with an embedded 1,10-phenanthroline moiety: fluorescent magnesium (II) ion sensor. Angew Chem Int Ed 2010;49:91–4.
[40] Song KC, Choi MG, Ryu DH, Kim KN, Chang SK. Ratiometric chemosensing of Mg^{2+} ions by a calix[4]arene diamide derivative. Tetrahedron Lett 2007;48:5397–400.
[41] Fu Z-H, Han X, Shao Y, Fang J, Zhang Z-H, Wang Y-W, Peng Y. Fluorescein-based chromogenic and ratiometric fluorescence probe for highly selective detection of cysteine and its application in bioimaging. Anal Chem 2017;89:1937–44.
[42] Jiang C, He W, Tai Z, Ouyang J. Spectral behavior and pH dependence of N-hexadecyl-5-iminomethyl-8-hydroxyquinoline. Spectrochim Acta, Part A 2000;56:1399–407.
[43] Yang X, Guo Y, Strongin RM. Conjugate addition/cyclization sequence enables selective and simultaneous fluorescence detection of cysteine and homocysteine. Angew Chem Int Ed 2011;50:10690–3.
[44] Farruggia G, Lotti S, Prodi L, Montalti M, Zaccheroni N, Savage PB, Trapani V, Sale P, Wolf FI. 8-Hydroxyquinoline derivatives as fluorescent sensors for magnesium in living cells. J Am Chem Soc 2006;128:344–50.
[45] Janakipriya S, Tamilmani S, Thennarasu S. A novel 2-(20-aminophenyl) benzothiazole derivative displays ESIPT and permits selective detection of Zn^{2+} ions: experimental and theoretical studies. RSC Adv 2016;6:71496–500.
[46] Park S-Y, Ghosh P, Park SO, Lee YM, Kwak SK, Kwon O-H. Origin of ultraweak fluorescence of 8-hydroxyquinoline in water: photoinduced ultrafast proton transfer. RSC Adv 2016;6:9812–21.
[47] Fu Z-H, Yan L-B, Zhang X, Zhu F-F, Han X-L, Fang J, Wang Y-W, Peng Y. A fluorescein-based chemosensor for relay fluorescence recognition of Cu(II) ions and biothiols in water and its applications to a molecular logic gate and living cell imaging. Org Biomol Chem 2017;15:4115–21.

[48] Wei G, Lin N, Gu Y, Ren X, Zhao G, Guang S, Feng J, Xu H. High selectivity improvement of chemosensors through hydrogen-induced emission (HIE) for detection of Hg2+ in vivo and in vitro. Sens Actuators, B 2020;321:128532.
[49] Fu Z-H, Wang Y-W, Peng Y. Two fluorescein-based chemosensors for the fast detection of 2,4,6-trinitrophenol (TNP) in water. Chem Commun 2017;53:10524–7.
[50] Gao J, Guo Y, Wang S, Deng T, Chen Y-W, Belzile N. Interference of lithium in measuring magnesium by complexometry: discussions of the mechanism. J Chem 2013:1–4. 2013.